

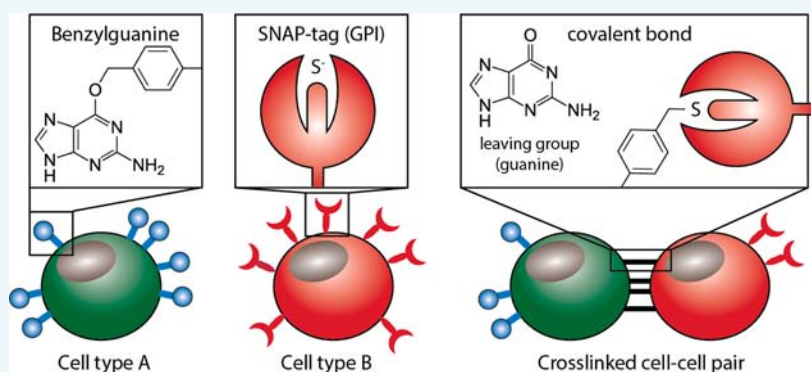
Capturing Cell–Cell Interactions via SNAP-tag and CLIP-tag Technology

S. Hoehnel[†] and M. P. Lutolf^{*,†,§}

[†]Laboratory of Stem Cell Bioengineering, Institute of Bioengineering, School of Life Sciences and School of Engineering and

[§]Institute of Chemical Sciences and Engineering, School of Basic Sciences, Ecole Polytechnique Fédérale de Lausanne, 1015 Lausanne, Switzerland

S Supporting Information



ABSTRACT: Juxtacrine or contact-dependent signaling is a major form of cell communication in multicellular organisms. The involved cell–cell and cell–extracellular-matrix (ECM) interactions are crucial for the organization and maintenance of tissue architecture and function. However, because cell–cell contacts are relatively weak, it is difficult to isolate interacting cells in their native state to study, for example, how specific cell types interact with others (e.g., stem cells with niche cells) or where they locate within tissues to execute specific tasks. To achieve this, we propose artificial in situ cell-to-cell linking systems that are based on SNAP-tag and CLIP-tag, engineered mutants of the human O6-alkylguanine-DNA alkyltransferase. Here we demonstrate that SNAP-tag can be utilized to efficiently and covalently tether cells to poly(ethylene glycol) (PEG)-based hydrogel surfaces that have been functionalized with the SNAP-tag substrate benzylguanine (BG). Furthermore, using PEG-based spherical microgels as an artificial cell model, we provide proof-of-principle for inducing clustering that mimics cell–cell pairing.

INTRODUCTION

Within native tissues, cells are physically constrained in three dimensions (3D) by adjacent neighboring and support cells as well as the architecture of the extracellular matrix (ECM). Cell–cell and cell–ECM interactions arise from these micro-environmental contacts and are important regulators of numerous biological functions such as tissue development, homeostasis, and regeneration.^{1–5} To probe the cellular organization within tissues, currently the only reliable technique is histotechnology, which involves fixation, sectioning, staining, and imaging of desired tissue samples.⁶ In addition to being time-consuming and expensive, histology cannot be applied to capture live cell interactions in a dynamic tissue environment. To overcome this technology gap, here we propose a fast and efficient in situ system to target and eventually isolate physically interacting neighboring cells of a given cell type using SNAP-tag or CLIP-tag technology.

SNAP-tag is a self-labeling protein tag that is a mutated form of the human suicide protein O6-alkylguanine-DNA alkyltransferase (hAGT), which was engineered by Johnsson and

colleagues to specifically and covalently bind O6-benzylguanine (BG) derivatives.⁷ Subsequently, a second mutant, CLIP-tag, was generated by the same group; this mutant reacts irreversibly and rapidly with O2-benzylcytosine (BC) derivatives.⁸ Together, the orthogonal relationship between the CLIP-tag and SNAP-tag systems can be exploited for simultaneous labeling with different probes.⁹

SNAP-tag has been developed for the efficient labeling of fusion proteins in living cells^{7,10,11} and has been validated for in vitro live fluorescent pulse–chase imaging.¹² Importantly, interference of SNAP-tag with protein function has been ruled out for various fusion proteins.^{7,13–17} The SNAP-tag substrate BG was historically developed as a potent anticancer drug for tumors showing augmented activity of human AGT.^{18,19} Pharmacologic studies on BG treatment could not link major side effects to its administration in mice, rats, or

Received: May 11, 2015

Revised: June 9, 2015

Published: June 16, 2015

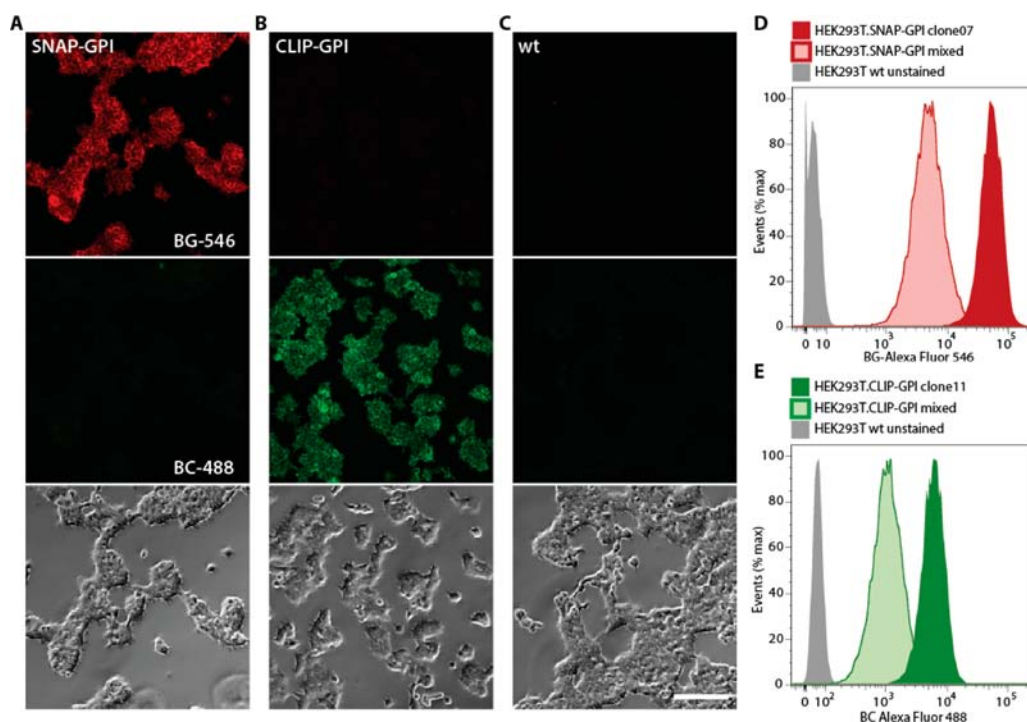


Figure 1. Expression of SNAP-tag and CLIP-tag on cell line HEK293T. (A–C) Fluorescence staining of SNAP-tag with BG-546 (red), CLIP-tag with BC-488 (green), and negative control (wild-type cells). (D and E) Flow cytometry analysis of selected high expressing clones for SNAP-tag (red) and CLIP-tag (green) on HEK293T. Scale bar is 100 μm .

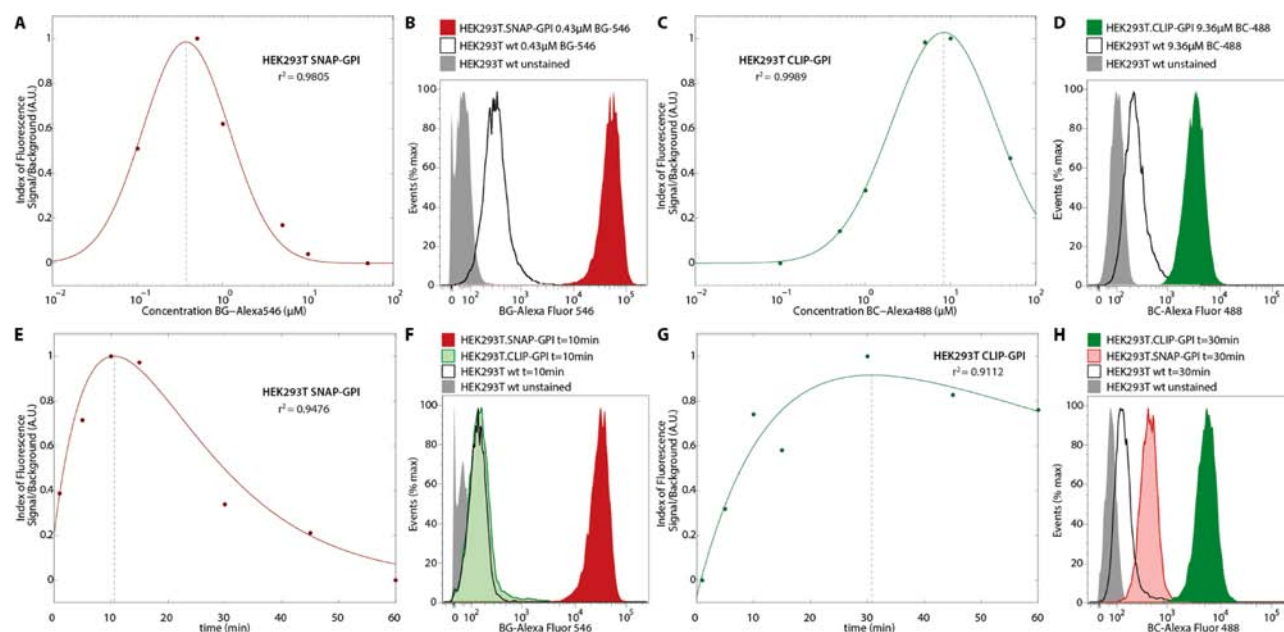


Figure 2. Optimal staining concentration and time for SNAP-tag and CLIP-tag. (A–D) A range of concentrations between 0.1 and 100 μM were tested to determine the optimal labelling concentration of the two substrates for labeling SNAP-tag and CLIP-tag present on the cell surface. (B and D) FACS analysis showed specific signal for SNAP–BG labeling (red) and CLIP–BC labeling (green) over background labeling of substrate attaching nonspecifically to wild-type cells (black outline). (E–H) Time points in the range of 1 min to 1 h were tested to determine the optimal time needed to label SNAP-tag and CLIP-tag present on the cell surface with their respective substrate BG and BC. (F) FACS analysis showed specific labeling of BG to surface-expressed SNAP–GPI (dark red) over unspecific binding to wild-type or CLIP–GPI-expressing cells (black outline and light green). (H) Similarly, BC specifically labeled surface-expressed CLIP–GPI (dark green) over unspecific binding to wild-type or SNAP–GPI-expressing cells (black outline and light red).

humans.^{20–22} To our knowledge, there are no studies addressing the potential side effects of the CLIP-tag substrate BC. However, BG and BC are structurally very similar, differing only in their respective leaving group, i.e., guanine versus

cytosine, which display similar pK_A values.²³ Therefore, one can comfortably posit that BC should not show any major pharmacologic adverse effects. Given these properties, SNAP-tag technology was proposed as an attractive system to sense

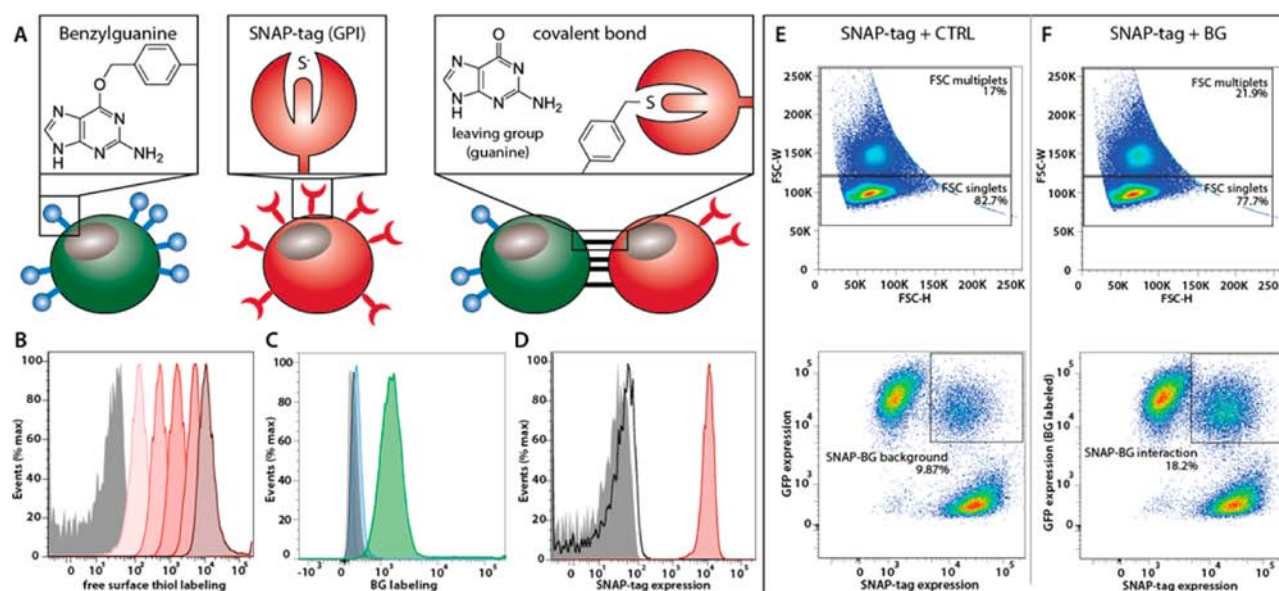


Figure 3. Targeting cell–cell pairing via SNAP–BG interactions. (A) In theory, cell–cell pairs can be formed through covalent bonds of SNAP-tag (red) with its substrate BG (blue) immobilized on the surface of cells (in green). (B) Free surface thiols are present on the surface of HEK293T cells as demonstrated by functionalization with Alexa546–maleimide at varying concentrations (gray, nonlabeled cells; red gradient histograms from left to right, cells labeled with 0.1, 1, 10, and 100 μ M and 1 mM). (C) These free-surface thiols can be targeted with maleimide-activated BG, whose presence is validated by labeling with SNAP–mCherry protein (green). The blue histogram shows wild-type HEK293T cells labeled with SNAP–mCherry. (D) SNAP-tag expression in HEK293T cells was confirmed by labeling with BG–Alexa546 (red). BG-labeled cells together with SNAP-tag-expressing HEK293T cells were incubated to form covalent cell bonds. (E) Singlet/multiplet flow cytometry plots for control samples where SNAP-tag-expressing cells were incubated with non-BG-labeled cells. (F) Singlet/multiplet flow cytometry plots for samples where SNAP-tag-expressing cells were incubated with BG-labeled cells.

and image not only protein–protein interactions inside living cells but also living organisms. Indeed, SNAP-tag has been employed for pulse–chase experiments to determine protein half-life in living mice.¹⁶

In this study, we extend the use of the SNAP-tag and CLIP-tag systems from the molecular level to the cellular level. We use SNAP-tag expressed globally and fused to a GPI anchor to successfully attach cells to culture surfaces on which they can be propagated. This opens up the possibility to create universal surfaces for nonadherent cells or cells whose adhesion ligands are unknown. Furthermore, we sought to apply the strategy to form covalent bonds between cells to permit custom cell–cell pairing and aggregation. As proof-of-principle, we utilized spherical PEG microgels functionalized with the SNAP-protein and SNAP-tag substrate BG, respectively, to form covalent bonds between microgels. This method should offer the possibility to isolate closely interacting cells, such as stem cells and their corresponding niche cells, in a completely unbiased fashion. One advantage of this system is the ability to isolate, without markers, a cell population of interest through another cell type whose phenotype is unknown.

RESULTS

Exclusive in Vitro Expression of SNAP-tag and CLIP-tag. We tested the efficiency and specificity of SNAP-tag or CLIP-tag expression and labeling on HEK293T cells (Figure 1). To this end, we generated stable cell lines using lentiviral vectors expressing either SNAP-tag or CLIP-tag fused to the glycosylphosphatidylinositol (GPI) signal sequence of human CD59 (pFUT.SNAP-GPI or pFUT.CLIP-GPI, respectively) from the ubiquitin C promoter.¹⁶ The CLIP-GPI construct²⁴ was inserted into the lentiviral pFUT vector using the AgeI and BspEI restriction sites. Using an anti-SNAP-tag antibody that

recognizes both SNAP-tag and CLIP-tag, we generated monoclonal cell lines from sorted single cells of the high 5% population to select for the highest transgene expression. To verify the expression of SNAP–GPI and CLIP–GPI, we labeled cells in culture with either BG–546 (SNAP substrate) or BC–488 (CLIP substrate). Indeed, a cell-surface-specific signal for BG–546 was detected in cells harboring the SNAP–GPI transgene (Figure 1A,D) but not on the wild-type controls (Figure 1C,D) or the cell lines harboring the CLIP–GPI transgene (Figure 1B,D). Similarly, cell-surface-specific BC–488 labeling was detected in the CLIP–GPI cell line but not on wild-type cells or SNAP–GPI cell lines (Figure 1A–C,E).

Characterization of SNAP–GPI and CLIP–GPI. To evaluate the respective optimal labeling concentration for SNAP–GPI and CLIP–GPI, we stained the generated cell lines with varying concentrations of BG–546 or BC–488, depending on the tag, for 30 min according to manufacturer's instructions (Figure 2A–D). Fitted to Gaussian bell curves, the optimal staining concentration with the best signal-to-noise (background staining on wild-type cells) ratio was determined at 0.4 μ M BG–546 and 9.2–9.4 μ M BC–488. Above this concentration, only the background from the unbound probe increased.

Next, we investigated the optimal staining time for BG–546 and BC–488 at the determined concentrations by staining at different time points ranging from 1 to 60 min (Figure 2E–H). SNAP-tag can be efficiently labeled within 10–15 min, whereas CLIP–GPI on HEK293T cells requires a staining time of approximately 30 min. By costaining with BG–546 and BC–488, we assessed the specificity of the substrates to the respective tag (Figure 2F,H). Except for minimal background noise of BC–488 on HEK293T.SNAP-GPI, no significant

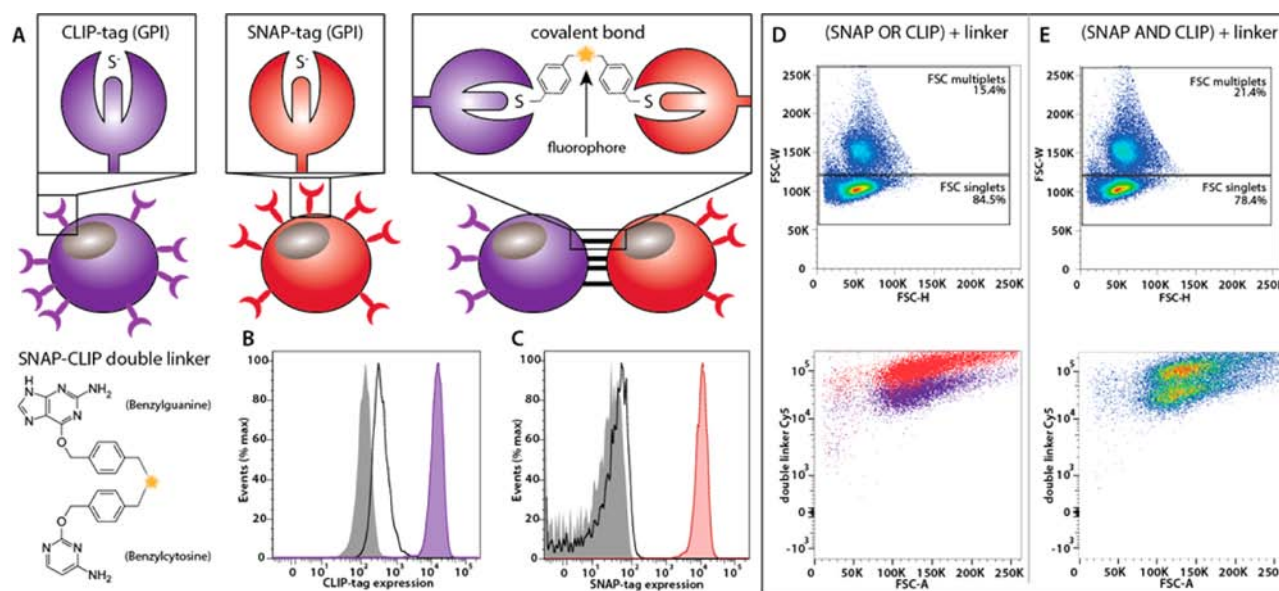


Figure 4. Targeting cell–cell pairing by using a heterobifunctional SNAP–CLIP linker. (A) Cell–cell pairs between CLIP-tag and SNAP-tag-expressing cells can be formed using the double functional linker molecule BG–Cy5–BC. (B) The BC active site can react with the CLIP-tag expressed on a GPI anchor on HEK293T cells to release cytosine, and (C) the BG active site can react with SNAP-tag also expressed on a GPI anchor on HEK293T cells. (D) As a control, either SNAP-tag cells or CLIP-tag cells were incubated alone with a Cy5-harboring double linker. (E) SNAP-tag and CLIP-tag cells were mixed together in one tube to observe through flow cytometry the formation of covalent bonds via the Cy5 fluorophore on the double linker.

unspecific staining on the respective orthogonal tag was measured.

BG Cell Surface Functionalization and Cell–Cell Pairing. For the first step in forming covalent cell–cell bonds using SNAP-tag technology (Figure 3A), cell surfaces must be functionalized with the SNAP-tag substrate BG. Naturally abundant free surface thiols pose an ideal target for binding thiol-reactive compounds, such as maleimide-functionalized molecules,²⁵ via Michael-type addition reaction. Indeed, by exploiting the presence of such reduced thiols on cellular surfaces, drug-loaded nanoparticles have been efficiently conjugated to donor cells to increase their therapeutic impact.²⁶ We confirmed the abundance of reduced surface thiols by functionalizing wild-type HEK293T with a variable concentration of maleimide-activated Alexa-fluor dyes (Figure 3B) and maleimide-activated BG (Figure 3C). Maleimide–Alexa-fluor546 was titrated at concentrations between 0.1 μ M and 1 mM. Within this range, we observed a constant increase of signal using flow cytometry, indicating that saturation of free surface thiols was not reached. BG was labeled to the cell surface similarly through maleimide–thiol coupling. The maximal concentration of BG in the labeling solution was 0.5 mM because of the solubility limit of BG in DMSO at 10 mM. A labeling solution of 0.5 mM corresponds to a final DMSO concentration of 5%, which is already 50-fold above standard cytotoxic limits.

Next, the presence and activity of BG after conjugation to the cell surface was verified by staining with SNAP–mCherry (Figure 3C). BG-labeled HEK293T-GFP cells were incubated together with stable SNAP-tag-expressing HEK293T cells that were labeled in red (Figure 3D) to investigate the formation of covalent bonds between these two cell types (Figure 3F). As a control, SNAP-tag-expressing cells were incubated with HEK293T-GFP cells that were not functionalized with BG–maleimide (Figure 3E). In general, we did not observe a marked increase in doublet or multiplet formation. However,

within the nonsinglet cell population, we observed a twofold increase of bonds between BG-functionalized cells and SNAP-tag-expressing HEK293T cells, reflected by the cell population that is fluorescent in both the green and red channels (Figure 3F).

These results suggest that SNAP-tag and its substrate BG each present on different cells cannot form sufficiently strong covalent bonds to induce and retain substantial levels of covalent cell–cell contacts. We speculate that this may be due to insufficient concentrations of either SNAP-tag or BG on the cells or from steric hindrance from other molecules present on the surface of cells.

Forming Artificial Cell–cell Bonds Using a Heterobifunctional Linker. Immobilized BG substrates can be withdrawn from cellular membranes through endocytic processes. Therefore, we investigated a different approach to forming artificial cell–cell bonds, namely, by utilizing a heterobifunctional linker harboring the SNAP-tag substrate BG on one end and the CLIP-tag substrate BC on the other end (Figure 4A).²⁷ Such a linker, bearing a Cy5 fluorescent dye in the center to allow fluorescent tracking by flow cytometry, was available at a concentration of 100 μ M (limited by the initial stock concentration). The specificity of this BG–Cy5–BC linker for SNAP-tag and CLIP-tag expressed on HEK293T cells was verified, and both tags are efficiently labeled within a 15 min incubation period (Figure S1).

We expected covalent cell–cell bonds to be formed by mixing a population of CLIP-tag-expressing cells (Figure 4B) and a population of SNAP-tag-expressing cells (Figure 4C). As a control, we incubated either SNAP-tag-expressing cells or CLIP-tag-expressing cells alone (Figure 4D). When incubating SNAP-tag- and CLIP-tag-expressing cells together (Figure 4E), we observed a slight increase (ca. 5%) in the nonsinglet cell population. However, within this population we could not observe any change in the formation of covalent bonds between SNAP-tag- and CLIP-tag-expressing cells. In theory, upon

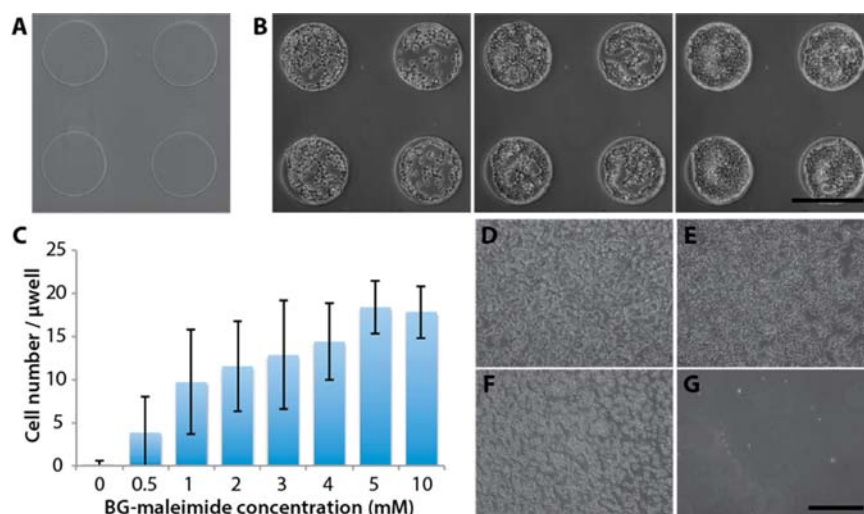


Figure 5. BG as a universal surface for SNAP-tag-expressing cells. (A) HEK293T wild-type cells and (B) HEK293T SNAP-tag-expressing cells were seeded on top of PEG hydrogel arrays functionalized with varying amounts of BG (C). (B) Snapshots of a time-lapse movie of HEK293T-SNAP-tag cells on PEG hydrogels functionalized with 5 mM BG at 0, 24, and 48 h (left to right, respectively). To validate the formation of covalent cell–cell bonds between SNAP-tag cells and the BG–PEG surface, (D) SNAP-tag cells seeded on 5 mM BG and (E) SNAP-tag cells seeded on 5 mM RGD were trypsinized for 15 min. (F) The SNAP-tag cells on BG remained attached, (G) whereas the SNAP-tag cells on RGD detached and were removed during a subsequent washing step. Scale bars are 500 μm .

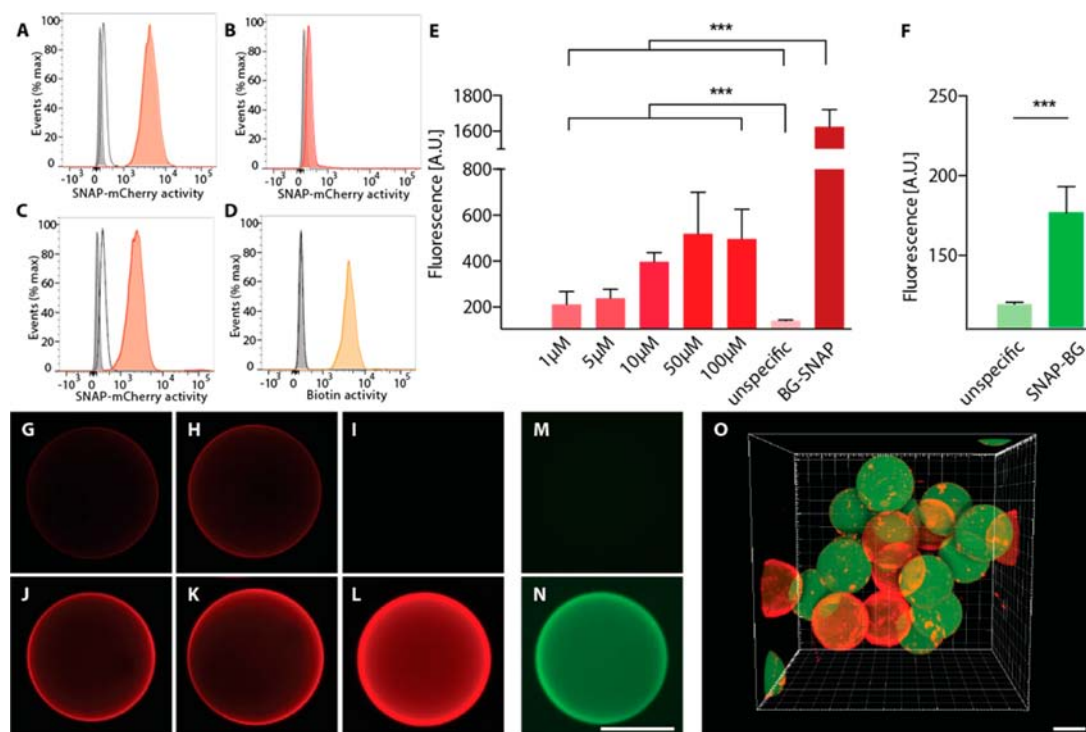


Figure 6. Formation of microgel clusters through SNAP technology. To imitate cell–cell clusters, we utilized PEG-based microbeads, on which concentrations of BG and SNAP protein can be maximized. (A–D) Functionalization of SNAP–mCherry protein for subsequent immobilization on PEG surfaces. BG-functionalized cells were stained with (A) wild-type SNAP–mCherry, (B) PEGylated SNAP–mCherry, and (C) biotinylated SNAP–mCherry (SNAP–mCherry–biotin). (D) Staining of SNAP–mCherry–biotin with streptavidin–Pacific orange. (E) Varying concentrations of SNAP–mCherry–biotin were immobilized on neutravin-functionalized microbeads (NA-microbeads). “Unspecific” refers to the fluorescence signal from SNAP–mCherry–biotin on microbeads without NA. “BG-SNAP” refers to the labeling of SNAP–mCherry on BG-functionalized microbeads. (F) Activity of immobilized SNAP–mCherry–biotin was verified by labeling with BG–Alexa488. “Unspecific” refers to the background signal from BG–Alexa488 on NA-microbeads without SNAP–mCherry. (G–N) Representative images of NA-microbeads with (G) 1 μM , (H) 5 μM , (J) 10 μM , (K) 50 μM of SNAP–mCherry–biotin. (I) Unspecific staining of SNAP–mCherry–biotin on microbeads without NA. (L) SNAP–mCherry immobilized on BG-microbeads. (M) Unspecific staining of BG–Alexa488 on NA-microbeads. (N) SNAP–mCherry–biotin immobilized on NA-microbeads labeled with BG–Alexa488. (O) SNAP-microbeads (red) and BG-microbeads (green) form stable clusters through the formation of covalent bonds. Scale bar is 100 μm .

forming covalent bonds, the two populations observed in their single state (Figure 4D; bottom, red and purple) should merge into one population.

Multiple reasons can explain the inability to form covalent cell–cell bonds. On the one hand, either tag could be masked by membrane proteins and therefore inaccessible on the membrane of the cell or the concentration of the heterobifunctional linker is too low to form sufficient cell–cell bonds to keep cell doublets or multiplets bound together during manipulation. On the other hand, the length of the cross-linker may simply be too short to enable the linking of SNAP-tag expressing cells with enough proximity to CLIP-tag expressing cells.²⁸

SNAP-tag as Universal Cell Attachment Surface. To determine the concentration of BG needed to covalently couple cells to a given surface, we used PEG hydrogels^{29,30} functionalized with different concentrations of BG (500 μ M to 10 mM; above 10 mM BG precipitated on the PEG hydrogel) as a surface for SNAP-tag-expressing cells (Figure 5). We found that above 5 mM, efficient cell attachment of SNAP-tag-expressing HEK293T cells to the hydrogel surface was facilitated (Figure 5B,C). Wild-type HEK293T cells could not form attachment sites to immobilized BG (Figure 5A). Interestingly, the proliferation of SNAP-tag-expressing cells anchored on BG surfaces was not inhibited (Figure 5B).

To demonstrate that the observed cell attachment is indeed due to covalent bond formation between the SNAP-tag expressed on cells and the BG immobilized on the PEG hydrogel, we trypsinized SNAP-tag-expressing cells on BG-substrates (Figure 5D) and on surfaces that were functionalized with 5 mM of the adhesion ligand RGD (Figure 5E), which results in similar cell attachment. Under the SNAP–BG condition, cells remained attached to the PEG surface even after multiple washing steps (Figure 5F). In contrast, cells completely detached from SNAP–RGD hydrogel surfaces and were rapidly washed away (Figure 5G). These results suggest that the amount of SNAP-tag (or CLIP-tag) substrate previously immobilized on the cell surface or provided as a heterobifunctional linker was too low to induce the formation of stable cell–cell bonds.

Imitating Cell–Cell Capturing through Biofunctionalized Microgels. Because we could not observe the formation of covalent bonds between cells harboring SNAP-tag or CLIP-tag and their corresponding substrates, we wanted to prove the principle of forming covalent bonds between nonflat surfaces using spherical PEG microgels.³¹

First, to immobilize SNAP–mCherry protein on PEG surfaces, we investigated different biofunctionalization strategies. The activity of PEG-conjugated SNAP–mCherry protein was tested by staining BG-functionalized cells and analyzing fluorescent signals through flow cytometry (Figure 6A–D) in comparison with native SNAP–mCherry protein (Figure 6A). The PEGylation of a SNAP–mCherry protein with an NHS–PEG–maleimide linker resulted in a complete loss of bioactivity (Figure 6B) probably because of the loss of the cysteine in the active site of the protein by the maleimide. As a result, we employed a biotin–NHS linker for coupling biotin to the SNAP–mCherry molecules, confirmed by staining with fluorescent–streptavidin (Figure 6D). Biotin–streptavidin binding resulted in no loss of protein activity as shown in Figure 6C. Indeed, by immobilizing neutravidin(NA)–maleimide on PEG microbeads through thiol conjugation, we were able to functionalize NA-displaying surfaces with

increasing amounts of SNAP–mCherry–biotin (Figure 6E,G–K). The amount of immobilized SNAP–mCherry remained much lower than that of the 5 mM BG units (Figure 6L). The activity of immobilized SNAP–mCherry protein was verified by staining with fluorescently labeled BG–Alexa488 (Figure 6F,M,N).

Next, BG-labeled PEG microgels were incubated with SNAP–mCherry-functionalized PEG microbeads. A short centrifugation step was necessary to obtain dense aggregates of microgels, as shown in Figure 6O. These clusters displayed covalent binding of SNAP-tag to BG, illustrated through the mixed clusters of red and green microgels, and were resistant to breakage through rigorous physical pipetting.

DISCUSSION

Within their native tissue microenvironments, mammalian cells often closely interact with neighboring cells that express factors critically influencing their behavior. For instance, the crosstalk between stem cells and their support cells in the so-called stem cell niche is key for tissue maintenance and regeneration. Hematopoietic stem cells, responsible for the life-long production of the entire blood system, presumably form cell pairs with niche cells whose identity remains poorly characterized. In mice, it is believed that several populations of such niche cells exist in the bone marrow,^{32–35} but their biology is poorly studied, largely because of the lack of suitable markers and the difficulty of accessing the stem cells in their native niches to directly study their behavior for example via live cell imaging. To address this problem, here we explored the ability of SNAP and CLIP technology for marker-free and thus unbiased cell isolation that is based on physiologically formed cell–cell interactions.

Using SNAP-tag technology, we globally expressed SNAP and CLIP attached to a GPI anchor protein on HEK293T model cells. We were able to generate cell lines with high expression levels of the protein tags to allow efficient labeling with their respective substrates BG and BC with relatively low concentrations (i.e., micromolar range) within a few minutes. Furthermore, we made use of the abundance of free thiols on the cell membrane to immobilize these substrates globally on a second HEK293T cell population. We hypothesized that incubation of SNAP-tag-expressing cells and BG-labeled cells would lead to the formation of a dense cell pellet that could no longer be dissociated. Although such strong pellet formation could not be observed in any instance, we did notice a slight increase in doublet formation of cells and SNAP–BG interactions, as seen through flow cytometry analyses. In addition, we tested whether SNAP-expressing and CLIP-expressing cells could be covalently bound to each other using a heterobifunctional BG–BC linker. However, in this scenario, we only observed a slight increase in cell doublet formation, rather than the generation of a dense nondissociable cell pellet. We hypothesized that either the concentration of SNAP-tag or substrate BG is too low to form such covalent artificial cell bonds or that the reaction site of the SNAP-tag toward the BG substrate is masked by other molecules present on cell membranes.

To investigate the concentration range of BG needed for efficient SNAP-tag binding on cells, we immobilized BG at different concentrations on synthetic hydrogel surfaces. We observed that above 5 mM of BG, SNAP-tag-expressing HEK293T cells could be efficiently attached to these surfaces. Furthermore, we demonstrated that this interaction is covalent

and specific; trypsinization does not lead to cell detachment as compared to control cell adhesion conditions dependent on integrin–RGD interactions.

To systematically test the potential of covalent nonflat surface pairing, we used micrometer-scale PEG hydrogel beads that we functionalized with relatively high concentrations of BG and SNAP protein to maximize the availability of binding sites. Indeed, by forcing the gel beads to contact each other, we observed the formation of stable aggregates of SNAP-tag and BG-conjugated microgels. On the basis of this finding, we conclude that the concentrations of SNAP-tag and/or BG on the cell surfaces obtained in our experiments are too low to result in the formation of covalently stabilized cell–cell pairs. The steric hindrance of the two reactive sites could be a cause for this concentration limitation; the binding sites could simply not be physically available for the formation of covalent cell–cell bonds. Here we optimized the expression of SNAP-tag and CLIP-tag under the short GPI anchor protein through the generation of high-expression-level monoclonal cell lines. However, in future experiments, these tags could be fused to the end of longer surface receptors such as cell-adhesion-mediating CD proteins to ensure sufficient exposure of the tags.

In addition, BG functionalization of cells is currently limited by the stock concentration of this molecule in its solvent DMSO. Indeed, BG is a strongly nonpolar molecule and thus is poorly soluble in water. This limitation could be resolved by generating BG linkers with long PEG chains in the center, a very common practice to enhance solubility of molecules, especially in aqueous solutions. Furthermore, to increase the local concentration of BG on cellular surfaces, a potential solution could be branched BG linkers, where one thiol on the cell membrane could lead to the exposure of multiple BG molecules.

In summary, we investigated whether SNAP technology can be used for artificially imitating cell–cell contact either with a substrate of interest or in between cells. We demonstrate that SNAP–BG interactions can be used for the generation of a universal cell surface by binding SNAP-expressing cells to BG-functionalized PEG. The use of SNAP-tag technology is currently underdeveloped for use in direct cell–cell pairing, but we demonstrated that PEG-based microbeads can cluster through SNAP protein immobilized on one bead population and BG exposure on the other. SNAP technology can thus far be used for the covalent attachment of a SNAP-tag-expressing cell to any given surface functionalized with its substrate BG. The generation of a universal surface, as demonstrated in this work, could be useful for the attachment of cells where long-term contact of cells with a surface is needed (i.e. for 2D screenings in which washing steps are associated with cell loss). Additionally, this method could be used for the attachment of cells whose adhesion ligands are unknown. To use SNAP-tag technology for cell–cell pairing, which would add versatility to methods of cell tracking and isolation, further optimization is needed.

■ EXPERIMENTAL PROCEDURES

Plasmid Constructs. The plasmid containing pFUT.CLIP-GPI was generated by insertion of the CLIP sequence from pEGFP-F.CLIP-GPI³⁶ into pFut.SNAP-GPI¹⁶ using the restriction sites AgeI and BspEI. The plasmid containing pET51b.CLIP-mCherry was generated by excising the CLIP sequence from the CLIPf vector (NEB) using the restriction sites BsrGI and XhoI and cloning the generated CLIP insert

into the pET51b.SNAP-mCherry vector³⁷ by replacing the SNAP-encoding sequence using the restriction sites Acc65I and XhoI. DNA sequences were verified using Sanger sequencing (Microsynth).

Virus Production. Lentiviral particles for pFut.SNAP-GPI and pFut.CLIP-GPI were produced by transfecting HEK293T cells using Xtreme Gene HP transfection reagent. Supernatants were collected at hours post transfection, filtered through 0.22 μm filters, and concentrated 1000 \times using ultracentrifugation.

Cell Culture and Cell Lines. HEK293T were cultured in Dulbecco's modified Eagle's medium (DMEM; Gibco) supplemented with 2 mM Glutamax, 10% (v/v) fetal bovine serum (FBS, Gibco), 1 mM sodium pyruvate (Gibco), 5 mM HEPES (Gibco) and 100 U mL⁻¹ penicillin/streptomycin (Invitrogen). The cells were stably transfected using pFut.SNAP-GPI and pFut.CLIP-GPI concentrated virus titers. Transfected cells were FACS sorted using rabbit polyclonal anti-SNAP-tag antibody (NEB, recognizing both SNAP-tag and CLIP-tag) at 1:200 and secondary Alexa-647-labeled goat anti-rabbit antibody (Invitrogen) at 1:1000. In a second round of FACS sorting, cells were labeled with BG-488 or BC-488 in addition to anti-SNAP-tag antibody labeling, and single cells of the high 5% positive-stained population were sorted into 96-well plates to generate monoclonal cell lines for each SNAP-tag and CLIP-tag. Monoclonal SNAP-tag and CLIP-tag cell lines were chosen according to proliferation rate and tag expression on the basis of labeling with BG-488 and BC-488.

Protein Expression and Purification. To express SNAP-mCherry, the constructs were transformed into Rosetta-gami (DE3) competent cells. Bacterial cultures harboring the expression construct were grown in LB broth containing 100 $\mu\text{g/mL}$ ampicillin (AppliChem) at 37 $^{\circ}\text{C}$ overnight under constant shaking. Overnight cultures of bacterial cells were diluted 100-fold into 2 L of LB broth supplemented with ampicillin and cultured as above until an OD₆₀₀ of 0.4–0.6 was reached. The culture was subsequently cooled to 16 $^{\circ}\text{C}$, induced by adding isopropyl-D-galactopyranoside (IPTG) to a final concentration of 1 mM, and additionally grown overnight at 16 $^{\circ}\text{C}$ under constant shaking. After harvesting by centrifugation at 4000 g for 10 min at 4 $^{\circ}\text{C}$, bacterial pellets were resuspended in IMAC lysis buffer supplemented with 1 mg/mL lysozyme and sonicated 3 times for 30 s on ice. After centrifugation at 12 000 g for 10 min to remove insoluble materials, the supernatant was purified by Ni-NTA Agarose chromatography according to manufacturer's instructions (Qiagen). Purified proteins were dialyzed against binding buffer (150 mM NaCl, 25 mM sodium phosphate, pH 8.0) and concentrated to working concentrations using Ultra-4 10K centrifugal filters (Amicon).

Microgel Generation. Computer-controlled syringe pumps (neMESYS from Cetoni, Germany) were used to control flow rates. Syringes were filled with PEG solutions, and hexadecane with 2% (w/v) ABIL EM surfactant was used as the oil phase. Tygon tubing was used to connect the syringes to the microfluidic chip inlets. Microgels were generated by loading two microfluidic channels with PEG precursors at concentrations depending on a specified molar excess of functional groups: for a 20% thiol excess, we chose 8.33% (w/v) PEG-VS and 20% (w/v) PEG-TH precursors. Microgels had a diameter of 120 μm . The oil phase was removed by filtering microgels with 70 μm cell strainers (BD Biosciences, USA) and extensive washing with PBS. Microgels were then swollen in PBS overnight. Microgels were subsequently incubated with 5 mM

BG–maleimide (in 50% DMSO) to generate BG-microgels or with 5 mM neutravidin–maleimide (in 50% DMSO) to generate neutravidin-functionalized microgels (NA-microgels). After either functionalization step, microgels were washed extensively with PBS on 40 μ m cell strainers.

Immobilization of SNAP–mCherry. To immobilize SNAP–mCherry protein on artificial surfaces, the protein was conjugated with a threefold molar excess of a 3.5 kDa NHS–PEG–maleimide linker (PEGylation) or a threefold molar excess of a 341.38 Da biotin–NHS linker (biotinylation) for 60 min at room temperature. PEGylated SNAP–mCherry could be immobilized by covalent interaction of the maleimide group with free thiols on PEG surfaces. Biotinylated SNAP–mCherry (SNAP–mCherry–biotin) was immobilized on PEG surfaces through interaction with surface-functionalized neutravidin–maleimide.

Statistical Analysis. For two-group analysis, an unpaired nonparametric Kolmogorov–Smirnov test was used. For all cases, *p* values less than 0.05 were considered statistically significant. GraphPad Prism 6.0 software was used for all statistical evaluations.

■ ASSOCIATED CONTENT

■ Supporting Information

The Supporting Information is available free of charge on the ACS Publications website at DOI: 10.1021/acs.bioconjchem.5b00268.

■ AUTHOR INFORMATION

Corresponding Author

*Tel.: +41216931876. E-mail: matthias.lutolf@epfl.ch. Laboratory of Stem Cell Bioengineering, Station 15, CH-1015 Lausanne, Switzerland.

Notes

The authors declare no competing financial interest.

■ ACKNOWLEDGMENTS

We thank Kai Johnsson, Luc Reymond, and Monica Rengifo Gonzalez for their help and time for discussions as well as for generously providing SNAP-tag products. We also thank Simone Allazetta for generating the PEG microgels. This work was funded by an ERC grant (StG_311422), a Swiss National Science Foundation Singergia grant (CRSII3_147684), the EU framework 7 HEALTH research programme PluriMes (<http://www.plurimes.eu/>), and the SystemsX.ch RTD project StoNets.

■ REFERENCES

- (1) Bhatia, S. N., Balis, U. J., Yarmush, M. L., and Toner, M. (1999) Effect of cell-cell interactions in preservation of cellular phenotype: cocultivation of hepatocytes and nonparenchymal cells. *FASEB J.* 13, 1883–1900.
- (2) Bazzoni, G., and Dejana, E. (2004) Endothelial cell-to-cell junctions: molecular organization and role in vascular homeostasis. *Physiol. Rev.* 84, 869–901.
- (3) Nelson, C. M., and Bissell, M. J. (2006) Of extracellular matrix, scaffolds, and signaling: tissue architecture regulates development, homeostasis, and cancer. *Annu. Rev. Cell Dev. Biol.* 22, 287–309.
- (4) Do, D. V., Mukhopadhyay, A., Lim, I. J., and Phan, T. T. (2007) The role of epithelial-mesenchymal interactions in tissue repair, fibrogenesis and carcinogenesis. *Curr. Signal Transduction Ther.* 2, 214–220.
- (5) Lodish, H., Berk, A., Zipursky, S., Matsudaira, P., Baltimore, D., and Darnell, J. (2000) Cell Interactions in Development, in *Molecular Cell Biology*, 4th ed., W. H. Freeman, New York.
- (6) Junqueira, L. C. U., Carneiro, J., and Contopoulos, A. N. (1975) *A Concise Medical Library for Practitioner and Student*, pp v, Lange Medical Publications, Los Altos, CA.
- (7) Keppler, A., Gendreizig, S., Gronemeyer, T., Pick, H., Vogel, H., and Johnsson, K. (2003) A general method for the covalent labeling of fusion proteins with small molecules in vivo. *Nat. Biotechnol.* 21, 86–89.
- (8) Gautier, A., Juillerat, A., Heinis, C., Correa, I. R., Jr., Kindermann, M., Beaufils, F., and Johnsson, K. (2008) An engineered protein tag for multiprotein labeling in living cells. *Chem. Biol.* 15, 128–136.
- (9) Provost, C. R., and Sun, L. (2010) Fluorescent labeling of COS-7 expressing SNAP-tag fusion proteins for live cell imaging. *J. Visualized Exp.*, No. e1876.
- (10) Keppler, A., Pick, H., Arrivoli, C., Vogel, H., and Johnsson, K. (2004) Labeling of fusion proteins with synthetic fluorophores in live cells. *Proc. Natl. Acad. Sci. U.S.A.* 101, 9955–9959.
- (11) Keppler, A., Arrivoli, C., Sironi, L., and Ellenberg, J. (2006) Fluorophores for live cell imaging of AGT fusion proteins across the visible spectrum. *BioTechniques* 41, 167–175.
- (12) Jansen, L. E., Black, B. E., Foltz, D. R., and Cleveland, D. W. (2007) Propagation of centromeric chromatin requires exit from mitosis. *J. Cell Biol.* 176, 795–805.
- (13) Maurel, D., Comps-Agrar, L., Brock, C., Rives, M. L., Bourrier, E., Ayoub, M. A., Bazin, H., Tinel, N., Durroux, T., Prezeau, L., Trinquet, E., and Pin, J. P. (2008) Cell-surface protein-protein interaction analysis with time-resolved FRET and snap-tag technologies: application to GPCR oligomerization. *Nat. Methods* 5, 561–567.
- (14) Hein, B., Willig, K. I., Wurm, C. A., Westphal, V., Jakobs, S., and Hell, S. W. (2010) Stimulated Emission Depletion Nanoscopy of Living Cells Using SNAP-Tag Fusion Proteins. *Biophys. J.* 98, 158–163.
- (15) Klein, T., Loschberger, A., Proppert, S., Wolter, S., van de Linde, S., and Sauer, M. (2011) Live-cell dSTORM with SNAP-tag fusion proteins. *Nat. Methods* 8, 7–9.
- (16) Bojkowska, K., Santoni de Sio, F., Barde, I., Offner, S., Verp, S., Heinis, C., Johnsson, K., and Trono, D. (2011) Measuring in vivo protein half-life. *Chem. Biol.* 18, 805–815.
- (17) Bodor, D. L., Rodriguez, M. G., Moreno, N., and Jansen, L. E. (2012) Analysis of protein turnover by quantitative SNAP-based pulse-chase imaging. In *Current Protocols in Cell Biology* (Bonifacio, J. S., Dasso, M., Lippincott-Schwartz, J., Harford, J. B., and Yamada, K. M., Eds.) Supplement 55, Unit 8.8, Wiley: New York.
- (18) Friedman, H. S., Kokkinakis, D. M., Pluda, J., Friedman, A. H., Cokgor, I., Haglund, M. M., Ashley, D. M., Rich, J., Dolan, M. E., Pegg, A. E., Moschel, R. C., McLendon, R. E., Kerby, T., Herndon, J. E., Bigner, D. D., and Schold, S. C., Jr. (1998) Phase I trial of O6-benzylguanine for patients undergoing surgery for malignant glioma. *J. Clin. Oncol.* 16, 3570–3575.
- (19) Quinn, J. A., Jiang, S. X., Reardon, D. A., Desjardins, A., Vredenburgh, J. J., Rich, J. N., Gururangan, S., Friedman, A. H., Bigner, D. D., Sampson, J. H., McLendon, R. E., Herndon, J. E., II, Walker, A., and Friedman, H. S. (2009) Phase II trial of Temozolomide plus o6-benzylguanine in adults with recurrent, Temozolomide-resistant malignant glioma. *J. Clin. Oncol.* 27, 1262–1267.
- (20) Dolan, M. E., Chae, M. Y., Pegg, A. E., Mullen, J. H., Friedman, H. S., and Moschel, R. C. (1994) Metabolism of O6-benzylguanine, an inactivator of O6-alkylguanine-DNA alkyltransferase. *Cancer Res.* 54, 5123–5130.
- (21) Chinnasamy, N., Rafferty, J. A., Hickson, I., Ashby, J., Tinwell, H., Margison, G. P., Dexter, T. M., and Fairbairn, L. J. (1997) O6-benzylguanine potentiates the in vivo toxicity and clastogenicity of Temozolomide and BCNU in mouse bone marrow. *Blood* 89, 1566–1573.
- (22) Wedge, S. R., Porteous, J. K., and Newlands, E. S. (1997) Effect of single and multiple administration of an O6-benzylguanine/

Temozolomide combination: an evaluation in a human melanoma xenograft model. *Cancer Chemother. Pharmacol.* 40, 266–272.

(23) Fasman, G. D. (1975) *Handbook of Biochemistry and Molecular Biology*, 3rd ed., CRC Press, Cleveland, OH.

(24) Gronemeyer, T., Chidley, C., Juillerat, A., Heinis, C., and Johnsson, K. (2006) Directed evolution of O6-alkylguanine-DNA alkyltransferase for applications in protein labeling. *Protein Eng., Des. Sel.* 19, 309–316.

(25) Sahaf, B., Heydari, K., Herzenberg, L. A., and Herzenberg, L. A. (2003) Lymphocyte surface thiol levels. *Proc. Natl. Acad. Sci. U.S.A.* 100, 4001–4005.

(26) Stephan, M. T., Moon, J. J., Um, S. H., Bershteyn, A., and Irvine, D. J. (2010) Therapeutic cell engineering with surface-conjugated synthetic nanoparticles. *Nat. Med.* 16, 1035–1041.

(27) Haruki, H., Gonzalez, M. R., and Johnsson, K. (2012) Exploiting Ligand-Protein Conjugates to Monitor Ligand-Receptor Interactions. *PLoS One* 7, No. 0037598.

(28) Sun, X. L., Dusserre-Bresson, F., Baker, B., Zhang, A. H., Xu, P., Fibbe, C., Noren, C. J., Correa, I. R., and Xu, M. Q. (2014) Probing homodimer formation of epidermal growth factor receptor by selective crosslinking. *Eur. J. Med. Chem.* 88, 34–41.

(29) Lutolf, M. P., and Hubbell, J. A. (2003) Synthesis and physicochemical characterization of end-linked poly(ethylene glycol)-co-peptide hydrogels formed by Michael-type addition. *Biomacromolecules* 4, 713–722.

(30) Gobaa, S., Hoehnel, S., Roccio, M., Negro, A., Kobel, S., and Lutolf, M. P. (2011) Artificial niche microarrays for probing single stem cell fate in high throughput. *Nat. Methods* 8, 949–955.

(31) Allazetta, S., Hausherr, T. C., and Lutolf, M. P. (2013) Microfluidic synthesis of cell-type-specific artificial extracellular matrix hydrogels. *Biomacromolecules* 14, 1122–1131.

(32) Sugiyama, T., Kohara, H., Noda, M., and Nagasawa, T. (2006) Maintenance of the hematopoietic stem cell pool by CXCL12-CXCR4 chemokine signaling in bone marrow stromal cell niches. *Immunity* 25, 977–988.

(33) Mendez-Ferrer, S., Michurina, T. V., Ferraro, F., Mazloom, A. R., Macarthur, B. D., Lira, S. A., Scadden, D. T., Ma'ayan, A., Enikolopov, G. N., and Frenette, P. S. (2010) Mesenchymal and haematopoietic stem cells form a unique bone marrow niche. *Nature* 466, 829–834.

(34) Nakamura, Y., Arai, F., Iwasaki, H., Hosokawa, K., Kobayashi, I., Gomei, Y., Matsumoto, Y., Yoshihara, H., and Suda, T. (2010) Isolation and characterization of endosteal niche cell populations that regulate hematopoietic stem cells. *Blood* 116, 1422–1432.

(35) Ding, L., Saunders, T. L., Enikolopov, G., and Morrison, S. J. (2012) Endothelial and perivascular cells maintain haematopoietic stem cells. *Nature* 481, 457–462.

(36) Maurel, D., Banala, S., Laroche, T., and Johnsson, K. (2010) Photoactivatable and photoconvertible fluorescent probes for protein labeling. *ACS Chem. Biol.* 5, 507–516.

(37) Brun, M. A., Tan, K. T., Nakata, E., Hinner, M. J., and Johnsson, K. (2009) Semisynthetic fluorescent sensor proteins based on self-labeling protein tags. *J. Am. Chem. Soc.* 131, 5873–5884.